Soil Parameter Optimization of the NGI-ADP Constitutive Model for Bangkok Soft Clay

B. Ukritchon[1] and T. Boonyatee[2]
[1,2]*Department of Civil Engineering, Chulalongkorn University, Bangkok, Thailand*
E-mail: boonchai.uk@gmail.com

ABSTRACT: This paper studies the NGI-ADP soil model, which can realistically simulate the anisotropic undrained stress strain responses and undrained shear strengths of clays. The model requires direct input parameters of undrained shear strengths and failure shear strains, including triaxial compression test, triaxial extension test and direct simple shear. However, parametric studies in this paper clearly show that trial-and-error testing of some input parameters is necessary in order to determine the optimal set of input parameters. The paper proposes the equations of anisotropic stress strain curves of this soil model and the technique of soil parameter optimization so that the optimal set of input parameters can be determined automatically and efficiently. The technique of soil parameter optimization is based on the statistical approach of least squares where proposed stress strain curves are used to compute model predictions. Finally, the proposed technique of soil parameter optimization of the NGI-ADP model is employed to determine the optimal set of input parameters for Bangkok soft clay.

1. INTRODUCTION

In geotechnical engineering, it is generally accepted that natural clays exhibit anisotropic shear properties, including stress strain response as well as undrained shear strengths. These anisotropic properties depends mode of shearing or applied stress path such as laboratory testings of triaxial compression (TC), triaxial extension (TE), and direct simple shear (DSS). Since the major principal stresses of these tests vary from the vertical direction (TC) to about 45° (DSS) and to the horizontal direction (TE), simple understanding of anisotropic stress strain and strength responses of natural clays is that they a function of the direction of major principal stress to the vertical. Ladd and DeGroot (2003) presented anisotropic undrained shear strength of normally consolidated clay for those testings as well as anisotropic undrained Young's modulus at 50% (E_{50}).

In general, the anisotropy of soil is classified into inherent and induced anisotropy following the concepts adopted by many researchers (e.g. Casagrande and Carillo, 1944; Wong and Arthur, 1986; Oda and Nakayama, 1988). Inherent anisotropy is defined as a physical characteristic which is inherent in the material and entirely independent of applied stresses. In other words, inherent anisotropy is the result of the deposition process and grain characteristics which is not altered significantly during normal loading. On the other hand, induced anisotropy is defined as due exclusively to the strain associated with applied stresses. This classification of soil anisotropy separates the effects of soil structure developed at the micro level (preferred particle orientations and inter-particle forces), giving rise to inherent anisotropy and the effects of pre-straining causing induced anisotropy. The effects of cross anisotropy in undrained shear strength of clays are attributed to inherent anisotropy and their deposition histories.

Some important recent researchers studied on the anisotropic strength of soils and the effect of anisotropic strength on soil behaviours (e.g. Casagrande and Carillo, 1944; Davis and Christian, 1971; Baker and Desai, 1984; Oda and Nakayama, 1988; Shibuya et al., 2003; Li and Dafalias, 2004; Liu and Indraratna, 2011). Undrained strength envelope and its relationship between undrained shear strength (s_u) and the direction of the major principal stress to the vertical (β) was proposed by Casagrande and Carillo (1944) and Davis and Christian (1971), where two and three parameters are used to describe the undrained strength envelope, respectively. In addition, tensor parameters was also employed for describing the effect of anisotropy on the peak strength for geomaterials, including Baker and Desai (1984), Oda and Nakayama (1988), Shibuya et al. (2003), Li and Dafalias (2004). For those studies, it was assumed that the peak undrained shear strength is affected by the inherent anisotropy in the form of a tensor. The fundamental difference between those studies exists in the representation of the inherent anisotropy by tensor or vector. In addition, a general anisotropic failure criterion was also proposed by Liu and Indraratana (2011) using tensor parameters of three sets of weakness planes and their associated reduction factors.

For typical cohesive soils, undrained shearing strength of triaxial compression, s_{uTC} is the largest, but that of triaxial extension, s_{uTE} is the lowest, while that of direct simple shear, s_{uDSS} is in between those limits. A similar behaviour can be observed for E_{50}. In addition, failure shear strains are different for different shearing modes. The shearing mode TC requires smallest failure shear strain but the shearing mode TE requires largest shear strain, while the failure shear strain of DSS shearing mode falls in between.

However, there are some cases where undrained shearing strength of triaxial extension, s_{uTE} is not the lowest. Instead, that of direct simple shear, s_{uDSS} is the lowest, such as Connecticut Valley varved clays. Engineering properties of this varved clay were early pioneered by Sambhandharaksa (1977). Undrained strength anisotropy of this geological material arises from soil structure at the macro level of alternating layers of medium grey inorganic silt and darker silty clay giving rise to the minimum strength parallel to the horizontal plane than any other planes. Thus, the use of undrained shear strength in compression mode as commonly used in practice leads to unsafe analysis of foundations on this varved clay.

Figure 1 shows soil elements of a foundation and importance of stress strain and strength anisotropy of clays. It can be seen that each of soil element undergoes different modes of shearing or different stress paths. Soil elements underneath the foundation are sheared in active mode or triaxial compression (TC), but soil elements beyond the edge of foundation are sheared in passive mode or triaxial extension (TE). Lastly, soil elements under directly the foundation corner are sheared in direct simple shear model. In addition, the major principal stress rotates from the vertical to the horizontal in the radial shear zone between the fan zones extending from the corner of foundation. A more reliable and accurate undrained finite element analysis in terms of ground movement and stability requires a realistic anisotropic constitutive soil model which can accurately simulate stress strain strength response in a generalized mode of shearing.

Anisotropic behaviors of clays and applications of anisotropic undrained shear strength in stability analyses include the examples of research works such as the concept of strain compatibility (Koutsoftas and Ladd, 1985), clay anisotropy (Seah, 1990), stability evaluation of embankment (Ladd, 1991), stability of braced excavations (Su et al.,1998; Ukritchon et al., 2003).

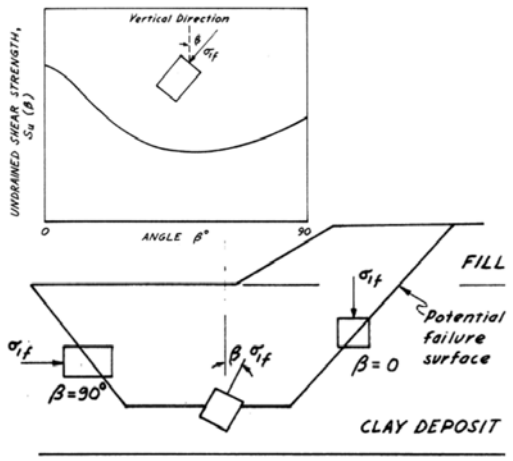

Figure 1 Soil elements of foundation in different modes of shearing (after Sambhandharaksa, 1977)

There are few constitutive soil models which can realistically simulate anisotropic stress strain responses and strength including the MIT-E3 model (Whittle, 1993), the MIT-S1 model (Pestana, 2012), the S-CLAY1S (Karstunen et al., 2005). Even they can model anisotropic variation in undrained stress strain and strength, those models do not use direct input of undrained shear strength. The anisotropic undrained shear strength is obtained from indirect relationship among several input parameters such as virgin compression compressibility, unloading-reloading compressibility, friction angle, over consolidation ratio, coefficient of lateral earth pressure at rest, etc. In addition, trial-and-error testing of several input parameters is necessary in order to calibrate the model to match undrained shear strength in different modes of shearing. Lastly, those models are still limited in research areas and are not available in commercial finite element codes in geotechnical practice.

Very recently, Grimstad et al. (2012) [10] have proposed the NGI-ADP constitutive soil mode whose key features are direct input parameter of undrained shear strength and failure shear strain in undrained tests of TC, TE, and DSS. Furthermore, this model is currently available in the commercial finite element code, PLAXIS2D (Brinkgreve, 2012). Thus, geotechnical engineers can apply it to accurately analyze undrained ground movement and stability problems in practice where anisotropic stress strain behaviors are considered in the analysis.

This paper presents parametric studies of important input parameters of this model in details. Then, the paper proposes equations of stress strain curves of this model and the technique of soil parameter optimization in efficiently determining the optimal set of input parameter of this model. The optimization technique eliminates trial-and-error testing of input parameter and obtains the optimal set of parameter automatically and efficiently. Lastly, the capability of the proposed technique of soil parameter optimization is demonstrated through examples of determining the optimal set of input parameters of the NGI-ADP model for Bangkok soft clay.

2. REVIEWS OF THE NGI MODEL

This section reviews the details of the NGI-ADP soil model concerning its input parameters and characteristic responses of stress strain strength anisotropy.

The NGI-ADP is based on the classical elasto-plastic constitutive model and formulated in terms of 3D generalized effective stress. The model is suitable for analyses of ground movement and stability in an undrained condition of cohesive soils. It generates anisotropic undrained stress strain responses and undrained shear strengths in generalized state of stress. The major input parameters are obtained from three undrained shear tests, and thus anisotropic responses of stress strain relationship in 3D generalized state of stress are completely defined. Figure 2 shows schematic diagrams of undrained stress strain curves generated by this model in three modes of shearing, including undrained tests of triaxial compression (TC), triaxial extension (TE), and direct simple shear (DSS). Table 1 summarizes a set of input parameters of this model. Some parameters in this table are also shown in Figure 2.

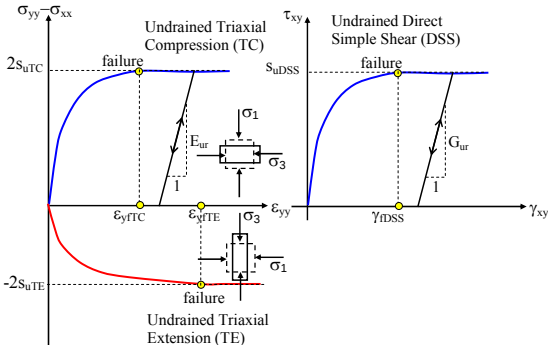

Figure 2 Stress strain curves generated by the NGI-ADP model

The NGI-ADP soil model requires 9 input parameters. Three pairs of parameters are used to independently match failure strains and undrained shear strength in TC, TE, and DSS. For TC tests, the parameters are: γ_{fc} and s_{uA}. For TE tests, the parameters are: γ_{fE} and s_{uP}. For DSS tests, the parameters are: γ_{fDSS} and s_{uDSS}. For both tests of TC and TE, the failure shear strain is equal to 3/2 of failure axial strain in TC (ε_{yfTC}) and TE (ε_{yfTE}), i.e. $\gamma_{fc} = 3\varepsilon_{yfTC}/2$, and $\gamma_{fE} = 3\varepsilon_{yfTE}/2$. It should be noted that the input undrained shear strengths correspond to the plane strain active condition (s_{uA}), plane strain passive condition (s_{uP}), and direct simple shear condition (s_{uDSS}). The model has the default relationship between undrained shear strength of triaxial compression (s_{uTC}) and that of active plane strain condition (s_{uA}) as: $s_{uTC} = 0.99 s_{uA}$. However, the model does not give any relationship between undrained shear strength of triaxial extension (s_{uTE}) and that of passive plane strain condition (s_{uP}).

Table 1 Input Parameters of the NGI Model

Symbol	Physical meaning	Type
G_{ur}	Unloading/reloading shear modulus	Stiffness
γ_{fC}	Shear strain at failure in triaxial compression	Stiffness
γ_{fE}	Shear strain at failure in triaxial extension	Stiffness
γ_{fDSS}	Shear strain at failure in direct simple shear	Stiffness
ν	Effective Poisson's ratio	Stiffness
s_{uA}	Active undrained shear strength (plane strain)	Strength
s_{uP}	Passive undrained shear strength (plane strain)	Strength
s_{uDSS}	Direct simple shear undrained shear strength	Strength
τ_0/s_{uA}	Initial shear mobilization	Initial stress

In addition to those parameters of different failure shear strains and undrained shear strengths, the model still requires the parameter of unloading and reloading shear modulus (G_{ur}), which is ones of the stiffness parameters. This parameter may be obtained from the slope of unloading and reloading path of stress strain curve of triaxial compression or direct simple shear tests. The latter test gives direct determination of G_{ur}, but the former test gives unloading and reloading Young's modulus (E_{ur}), where G_{ur} can be calculated as:

$$G_{ur} = \frac{E_{ur}}{2(1+\nu)} \quad (1)$$

It should be noted that unloading and reloading paths of TC or DSS tests are not typically carried out in such tests.

The model uses a single parameter which control initial stress condition of undrained loading. This parameter is the initial shear mobilization (τ_0/s_{uA}) which can be determined from the coefficient of lateral earth pressure at rest (K_0) and initial vertical effective stress (σ'_{yy}), as indicated in Table 1. In this paper, the paper concerns with the studies of isotropic initial stress condition, $K_0 = 1$. Accordingly, this input parameter, $\tau_0/s_{uA} = 0$.

The last input parameter of this model is the effective Poisson's ratio (ν). The model recommends the range of this parameter as 0.3-0.4. All results in the paper are obtained from calculations using ν = 0.3. According to PLAXIS's manual (Brinkgreve, 2012), the undrained stress strain curve is simulated such that the bulk modulus of water is used to compute the excess pore water pressure, while the NGI model is employed in an integration of the effective stress model. The bulk modulus used in this undrained analysis has a realistically high value in order to ensure that the idealized incompressible or undrained conditions are achieved in the analysis as if the total Poisson's ratio of 0.5 is used. The latter case is not recommended in this undrained analysis since such condition of the total Poisson's ratio of 0.5 or 0.495 may lead to ill-conditioning of the stiffness matrix and numerical problems.

In conclusion, characteristic responses of stress strain curves are nonlinear and anisotropic, where anisotropic behaviours of 3D generalized state of stress are completely defined by three undrained tests of TC, TE, and DSS. Stress strain curves of TC, TE, and DSS increase nonlinearly and monotonically and are the major keys in determination of crucial input parameters, especially failure shear strains and undrained shear strengths. In each mode of shearing, the failure happens when the shear strain reaches its corresponding failure shear strain and thus, the shear stress in that mode is fully mobilized to its own undrained shear strength.

A brief mathematical description of the NGI soil model is given below. Full mathematical formulations of this model can be found in Grimstad et al. (2012).

The yield criterion, F, of the NGI model is expressed as the 3D generalized effective state of stress by modifying the classical Tresca yield criterion so that it takes into account of anisotropic undrained shear strength as follows:

$$\mathrm{F} = \sqrt{\mathrm{H}\hat{\mathrm{J}}_2} - \kappa\frac{\mathrm{s_{uA}} - \mathrm{s_{uP}}}{2} = 0 \tag{2}$$

where

$$\mathrm{H} = \cos^2\left(\frac{1}{6}\arccos\left(1 - 2\mathrm{a}_1\omega\right)\right)$$

$$\omega = \frac{27}{4}\frac{\hat{J}_3^2}{\hat{J}_2^3}$$

$$\hat{J}_2 = -\hat{s}_{xx}\hat{s}_{yy} - \hat{s}_{xx}\hat{s}_{zz} - \hat{s}_{yy}\hat{s}_{zz} + \hat{s}_{xy}^2 + \hat{s}_{xz}^2 + \hat{s}_{yz}^2$$

$$\hat{J}_3 = -\hat{s}_{xx}\hat{s}_{yy}\hat{s}_{zz} + 2\hat{s}_{xy}\hat{s}_{yz}\hat{s}_{xz} - \hat{s}_{xx}\hat{s}_{yz}^2 - \hat{s}_{yy}\hat{s}_{xz}^2 - \hat{s}_{zz}\hat{s}_{xy}^2$$

$$\begin{bmatrix}\hat{s}_{xx}\\ \hat{s}_{yy}\\ \hat{s}_{zz}\\ \hat{s}_{xy}\\ \hat{s}_{xz}\\ \hat{s}_{yz}\end{bmatrix} = \begin{bmatrix}\left(\sigma'_{xx} - \sigma'_{xx0}\cdot\left(1-\kappa\right)\right) + \kappa\frac{1}{3}\left(s_{\mathrm{uA}} - s_{\mathrm{uP}}\right) - \hat{p}\\ \left(\sigma'_{yy} - \sigma'_{yy0}\cdot\left(1-\kappa\right)\right) + \kappa\frac{1}{3}\left(s_{\mathrm{uA}} - s_{\mathrm{uP}}\right) - \hat{p}\\ \left(\sigma'_{zz} - \sigma'_{zz0}\cdot\left(1-\kappa\right)\right) + \kappa\frac{1}{3}\left(s_{\mathrm{uA}} - s_{\mathrm{uP}}\right) - \hat{p}\\ \tau_{xy}\frac{s_{\mathrm{uA}} + s_{\mathrm{uP}}}{2s_{\mathrm{uDSS}}}\\ \tau_{xz}\\ \tau_{yz}\frac{s_{\mathrm{uA}} + s_{\mathrm{uP}}}{2s_{\mathrm{uDSS}}}\end{bmatrix}$$

$$\hat{p} = \frac{\left(\sigma'_{xx} - \sigma'_{xx0}\left(1-\kappa\right)\right) + \left(\sigma'_{yy} - \sigma'_{yy0}\left(1-\kappa\right)\right) + \left(\sigma'_{zz} - \sigma'_{zz0}\left(1-\kappa\right)\right)}{3}$$

$$= p' - \left(1-\kappa\right)p'_0$$

$$p' = \frac{\sigma'_{xx} + \sigma'_{yy} + \sigma'_{zz}}{3}$$

$$p'_0 = \frac{\sigma'_{xx0} + \sigma'_{yy0} + \sigma'_{zz0}}{3}$$

σ'_{xx0}, σ'_{yy0}, σ'_{zz0} are the initial stresses in x, y, z, respectively.

It should be noted that $\hat{J}_2$ *and* $\hat{J}_3$ are the modified second and third deviatoric invariants while the term k is the hardening parameter. The term a is the rounding factor of the modified Tresca yield criterion enabling the yield function to be continuous and differentiable at any state of stress, where a value of 0.97 is chosen as default. Geometrically, the yield criterion in the π plane is a translated, rounded hexagonal shape of the classical Tresca yield criterion.

The hardening parameter, κ is given by the following mathematical function as:

$$\kappa = 2\frac{\sqrt{\gamma^{\mathrm{P}}/\gamma_f^P}}{1+\gamma^P/\gamma_f^P} \text{ when } \gamma^P < \gamma_f^P \text{ else } \kappa = 1 \tag{3}$$

where

$$\gamma_f^P = \frac{\hat{R}_B\hat{R}_D\sqrt{\left(\hat{R}_D^2 - \hat{R}_c^2\right)\cos^2 2\hat{\theta} + \hat{R}_c^2} - \hat{R}_D^2\hat{R}_A^2\cos 2\hat{\theta}}{\hat{R}_B^2 - \left(\hat{R}_B^2 - \hat{R}_D^2\right)\cos^2 2\hat{\theta}}$$

$$\hat{R}_A = \frac{\gamma_{\mathrm{fE}} - \gamma_{\mathrm{fC}}}{2}$$

$$\hat{R}_B = \frac{\gamma_{\mathrm{fE}} + \gamma_{\mathrm{fC}}}{2}$$

$$\hat{R}_C = \sqrt{\gamma_{\mathrm{fE}}\gamma_{\mathrm{fC}}}$$

$$\hat{R}_D = \frac{\gamma_{\mathrm{fDSS}}\hat{R}_B}{\hat{R}_C}$$

$$\cos 2\hat{\theta} = \frac{\sqrt{3}}{2}\frac{\hat{\mathrm{s}}_{\mathrm{yy}}}{\sqrt{\hat{\mathrm{J}}_2}}$$

γ^{P} = plastic shear strain

The plastic shear strain is obtained from integration the incremental plastic shear strain, $\mathrm{d}\gamma^{\mathrm{P}}$ of the following expression:

$$\mathrm{d}\gamma^{\mathrm{P}} = \sqrt{\mathrm{H}}\sqrt{\frac{2}{3}\left[\left(\mathrm{d}\varepsilon_{\mathrm{xx}}^{\mathrm{P}} - \mathrm{d}\varepsilon_{\mathrm{yy}}^{\mathrm{P}}\right)^2 + \left(\mathrm{d}\varepsilon_{\mathrm{xx}}^{\mathrm{P}} - \mathrm{d}\varepsilon_{\mathrm{zz}}^{\mathrm{P}}\right)^2 + \left(\mathrm{d}\varepsilon_{\mathrm{yy}}^{\mathrm{P}} - \mathrm{d}\varepsilon_{\mathrm{zz}}^{\mathrm{P}}\right)^2\right] + \left(\mathrm{d}\gamma_{\mathrm{xy}}^{\mathrm{P}}\right)^2 + \left(\mathrm{d}\gamma_{\mathrm{xz}}^{\mathrm{P}}\right)^2 + \left(\mathrm{d}\gamma_{\mathrm{yz}}^{\mathrm{P}}\right)^2} \tag{4}$$

The NGI soil model employs the non-associated flow rule giving rise to the incremental plastic strain, $\mathrm{d}\varepsilon^{\mathrm{P}}$, and the corresponding derivative of the plastic potential, $\frac{\partial Q}{\partial \sigma'}$, as follows:

$$\mathrm{d}\varepsilon^{\mathrm{P}} = \mathrm{d}\lambda\frac{\partial Q}{\partial \sigma'} \tag{5}$$

$$\frac{\partial Q}{\partial \sigma'} = \frac{1}{2}\left(\hat{1} + \frac{\partial p}{\partial \sigma'} \left\{ \frac{\partial \hat{s}}{\partial \hat{p}} \right\}^T \right) \frac{\partial \hat{J}_2}{\partial \hat{s}} \sqrt{\frac{1}{\hat{J}_2}} \qquad (6)$$

where

$$\hat{1} = \left[1 \quad 1 \quad 1 \quad \frac{s_{uA} - s_{uP}}{2s_{uDSS}} \quad 1 \quad \frac{s_{uA} - s_{uP}}{2s_{uDSS}} \right]$$

$d\lambda$ = plastic multiplier

Finally, the incremental elastic strain of NGI soil model follows a conventional incremental elasto plastic model (e.g. Potts and Zdravkovic, 1999) and the decomposition concept of the total incremental strain as the sum of incremental elastic strain the incremental plastic strain. The above description concludes a concise mathematical description of the NGI soil model.

3. PARAMETRIC STUDIES OF INPUT PARAMETERS

In order to avoid any error from numerical integration of constitutive equation of this model or from finite element modelling in setting up TC, TE and DSS tests, the paper obtains the data of stress strain curves from the model by using the utility tool, PLAXIS SoilTest, which is available in PLAXIS2D. This utility can easily generate stress strain curves of predefined laboratory tests including TC, TE and DSS in undrained shearing conditions without setting corresponding finite element modelling. Thus, it ensures that the paper has correctly and accurately obtained the data of stress strain curves of TC, TE, and DSS tests, which are used to carry out several parametric studies and to develop proposed equations of stress strain curves of the NGI-ADP model in the next section.

Figures 3-5 show influence of term G_{ur}/s_{uA} to the normalized stress strain curves of TC, TE, and DSS, respectively. For normalized plots of TC and TE tests, the horizontal axis is the ratio of axial strain to the failure axial strain of each test ($\varepsilon_{yy}/\varepsilon_{yfTC}$, $\varepsilon_{yy}/\varepsilon_{yfTE}$) or shear strain to the failure shear strain (γ_{TC}/γ_{fC}, γ_{TE}/γ_{yE}), while the vertical axis is the ratio of maximum shear stress to the undrained shear strength of each test ($(\sigma_1-\sigma_3)/2s_{uTC}$, $(\sigma_1-\sigma_3)/2s_{uTE}$). For DSS plot, the horizontal axis is the ratio of shear strain to the failure shear strain ($\gamma_{xy}/\gamma_{fDSS}$), while the vertical axis is the ratio of shear stress to the DSS undrained shear strength (τ_{xy}/s_{uDSS}). In other words, the horizontal axes represent shear strain normalized to its corresponding failure strain while the vertical axes represent shear stress normalized to it corresponding strength. As a result, all horizontal and vertical axes of the normalized stress strain curve have the range of 0-1. The points where normalized values reach unity indicate the state of failure.

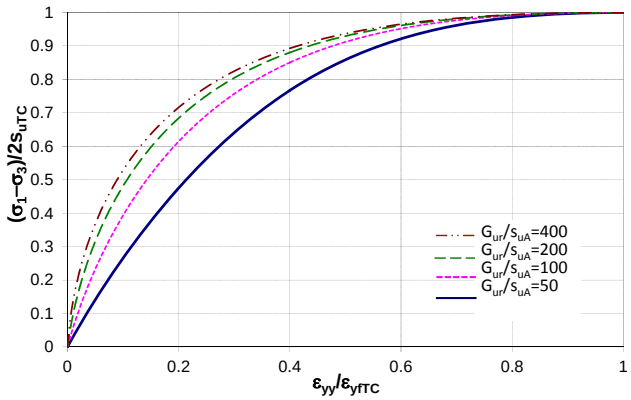

Figure 3 Effect of G_{ur}/s_{uA} to normalized stress strain curves of TC

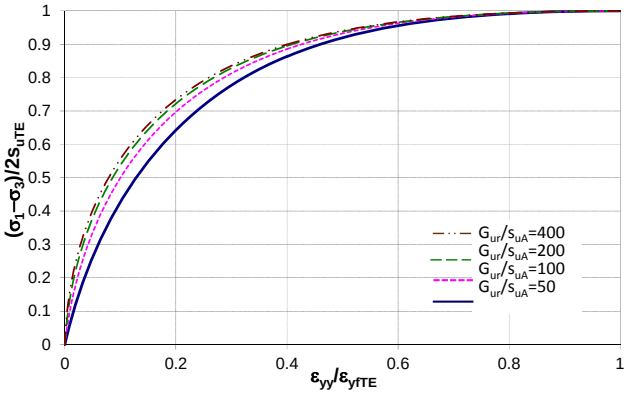

Figure 4 Effect of G_{ur}/s_{uA} to normalized stress strain curves of TE

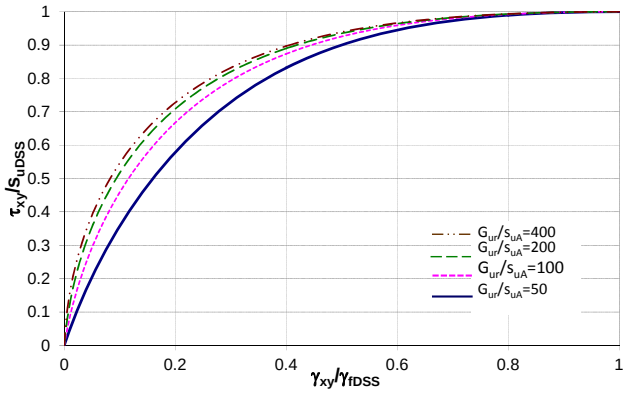

Figure 5 Effect of G_{ur}/s_{uA} to normalized stress strain curves of DSS

It should be noted that by presenting stress strain curves in normalized axes as explained above, number of parameters affecting the model can be systematically reduced. As a result, conclusion of parametric studies can be clearly drawn and generalized.

It can be seen from those figures that the term G_{ur}/s_{uA} affects the curvature of normalized stress strain curve for all shearing paths, TC, TE, and DSS. In general, it can be observed that larger values of G_{ur}/s_{uA} cause stiffer response of stress strain curve for all tests.

Figures 6-8 show influence of failure shear strain, γ_{fC}, γ_{fE}, γ_{fDSS} to the normalized stress strain curves of TC, TE, and DSS, respectively. It can be observed that failure shear strain of each mode affects its own curvature of normalized stress strain curve. The effect of failure shear strain is similar to that of G_{ur}/s_{uA}. The normalized stress strain curve tends to be stiffer as the failure shear strain increases for all modes of shearing.

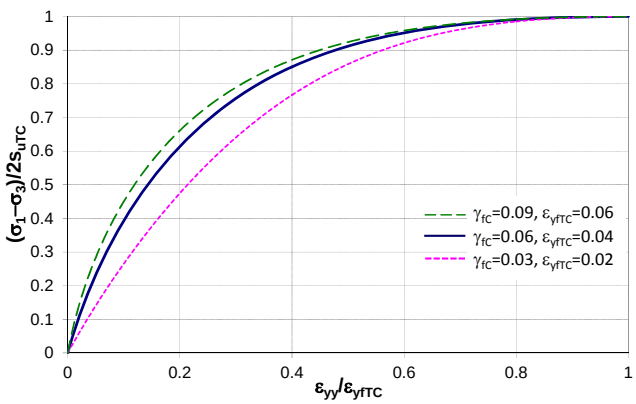

Figure 6 Effect of γ_{fc} to normalized stress strain curves of TC

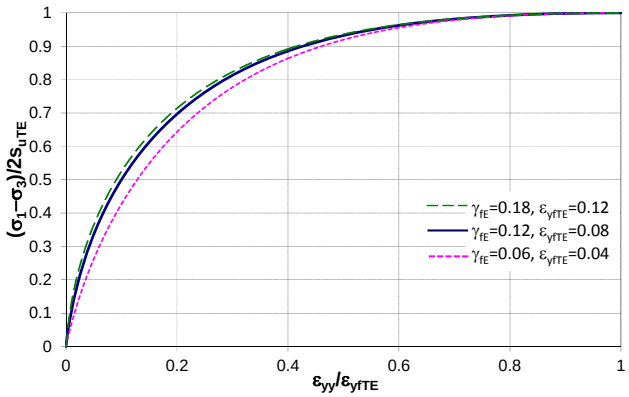

Figure 7 Effect of γ_{fE} to normalized stress strain curves of TE

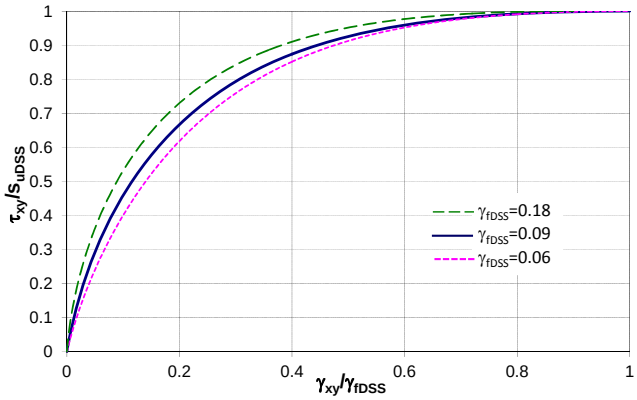

Figure 8 Effect of γ_{fDSS} to normalized stress strain curves of DSS

Figure 9 shows comparisons of normalized stress strain curves between TC, TE and DSS, where G_{ur}/s_{uA} = 200, γ_{fC} = 0.04, γ_{fE} = 0.15, γ_{fDSS} = 0.07. It can be seen that the normalized stress strain curve are not unique to each other. The normalized stress strain curve of TE test is the stiffest, but that of TC test is the softest, while that of DSS test falls in between. This result suggests that stress strain curve of each mode is not unique to each other.

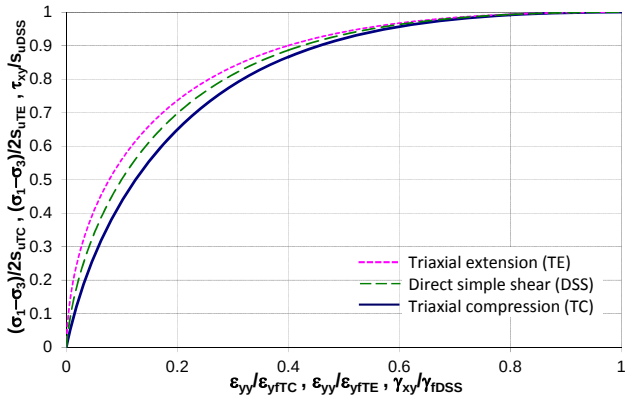

Figure 9 Normalized stress strain curve between TC, TE, and DSS

The last parametric study of the NGI-ADP model is the relationship between s_{uTE} and s_{uP}, which are not clearly mentioned in the model formulation. It should be noted that the mathematical formulation of this model set the relationship between the TC undrained shear strength (s_{uTC}) and the active plane strain undrained shear strength (s_{uA}) as: $s_{uTC} = 0.99 s_{uA}$. However, the formulation did not give any relationship between the TE undrained shear strength (s_{uTE}) and the passive plane strain undrained shear strength (s_{uP}). It may be reasonable to assume the condition that: $s_{uTE} = s_{uP}$. However, a clear relationship should be figure out in order to obtain a better model calibration. Figure 10 shows the parametric study of latter relationship. It can be observed that there is linear relationship between s_{uTE}/s_{uA} and s_{uP}/s_{uA} as:

$$s_{uTE} = s_{uP} - 0.01 s_{uA} \tag{7}$$

This result indicates that inter-relationship between s_{uTE}, s_{uP}, and s_{uA} has small influence on the model calibration in getting a more accurate value of input parameter of passive plane strain undrained shear strength.

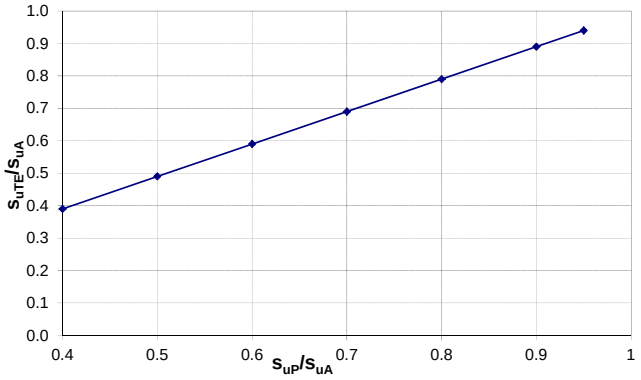

Figure 10 Inter-relationship between s_{uTE}, s_{uP}, s_{uA}

In sum, even though parameters of failure strains and undrained shear strengths of the NGI-ADP model can be determined directly from TC, TE, and DSS test, results of parametric studies of those parameters indicate that determining the optimal set of input parameter still require process of trial-and-error testing of parameters in order to closely match the predicted stress strain responses and strengths with the laboratory data of TC, TE, and DSS. This is because the curvature of stress strain curve of each mode of shearing (TC, TE, DSS) depend on both the ratios of unloading/reloading shear modulus to the active plane strain shear strength (G_{ur}/s_{uA}) and failure shear strain in each test (γ_{fC}, γ_{fE}, γ_{fDSS}). Furthermore, parameters of undrained shear strengths in different modes of shearing (s_{uTE}, s_{uP}, and s_{uA}) have inter-relationship.

Therefore, the technique of soil parameter optimization may be adopted in order to obtain the optimal set of input parameters of the NGI-ADP soil model which best fit the predictions with the soil data. However, before applying the technique of soil parameter optimization, closed-form stress strain curves must be determined.

4. PROPOSED EQUATIONS OF STRESS STRAIN CURVES FOR THE NGI-ADP MODEL

Due to mathematical complexity of the NGI-ADP model, analytical closed-form expressions of stress strain curve cannot be derived explicitly. Instead, stress strain data by this model must be obtained by means of numerical integration of constitutive equation using the standard method of elasto-plastic model such as explained by Potts and Zdravkovic (1999). Nonetheless, it is not possible to determine analytical closed-form expressions of stress strain curves of this model.

In addition to integration procedure of constitutive equation, the stress strain data of the NGI-ADP model can be obtained through data generation by PLAXIS SoilTest as explained earlier. However, such processes are not convenient and practical with the technique of soil parameter optimization since the model prediction of stress strain results must be calculated independently within the optimization formulation. Therefore, closed-form expression of stress strain curves must be clearly determined such that the technique of soil parameter optimization can be implemented very efficiently.

The paper proposes stress strain equations of TC, TE, and DSS tests for the NGI-ADP model as follows:

$$TC: \frac{(\sigma_1-\sigma_3)}{2s_{uTC}} = \frac{A\frac{\varepsilon_{yy}}{\varepsilon_{yfTC}} + B\sqrt{\frac{\varepsilon_{yy}}{\varepsilon_{yfTC}}} + C\left(\frac{\varepsilon_{yy}}{\varepsilon_{yfTC}}\right)^2}{D\frac{\varepsilon_{yy}}{\varepsilon_{yfTC}} + 1} \quad (8)$$

$$TE: \frac{(\sigma_1-\sigma_3)}{2s_{uTE}} = \frac{E\frac{\varepsilon_{yy}}{\varepsilon_{yfTE}} + F\sqrt{\frac{\varepsilon_{yy}}{\varepsilon_{yfTE}}} + G\left(\frac{\varepsilon_{yy}}{\varepsilon_{yfTE}}\right)^2}{H\frac{\varepsilon_{yy}}{\varepsilon_{yfTE}} + 1} \quad (9)$$

$$DSS: \frac{\tau_{xy}}{s_{uDSS}} = \frac{J\frac{\gamma_{xy}}{\gamma_{fDSS}} + K\sqrt{\frac{\gamma_{xy}}{\gamma_{fDSS}}} + L\left(\frac{\gamma_{xy}}{\gamma_{fDSS}}\right)^2}{M\frac{\gamma_{xy}}{\gamma_{fDSS}} + 1} \quad (10)$$

where A, B, C, D = f(G_{ur}/s_{uA}, γ_{fC})
E, F,G, H = f(G_{ur}/s_{uA}, γ_{fE})
J, K, L, M = f(G_{ur}/s_{uA}, γ_{fDSS})
$\gamma_{fC} = 3\varepsilon_{yfTC}/2$
$\gamma_{fE} = 3\varepsilon_{yfTE}/2$

It should be noted that each equation of stress strain curve use four coefficients. Coefficient terms (A-D), (E-H), (J-M) are not constant, but functions of G_{ur}/s_{uA}, and failure shear strains (γ_{fC}, γ_{fE}, γ_{fDSS}) of TC, TE, and DSS tests, respectively. Because each set of coefficients have very complex mathematical form, their expression are not given here. For stress strain curves of TC and TE, shear stresses are normalized by their corresponding shear strengths, namely s_{uTC}, and s_{uTE}, instead of active and passive plane strain shear strength, s_{uA}, and s_{uP}, which are the direct input parameter of the model.

Several mathematical functions were tested whether they can best fit the data of stress strain curve. Those functions include polynomial, exponential, power, logarithm, hyperbola, and rational functions. Equations (8)-(10) are the final best mathematical functions in the form of rational expression. In addition, the ranges of studied normalized parameters cover most real soil behaviours, where G_{ur}/s_{uA}=50-1000, failure shear strains, γ_{fC}, γ_{fE}, γ_{fDSS} = 0.001-0.3. Figure 11 shows schematic diagram of an example of normalized stress strain curve in any test. Basically, the curve increases monotonically from 0 and reaches unity at failure for both the normalized shear strain and normalized shear stress. Thus, equation of each stress strain curve can be casted in a generalized function as:

$$f = \frac{a_1 x + a_2\sqrt{x} + a_3(x)^2}{a_4 x + 1} \quad (11)$$

where f = normalized shear stress
x = normalized shear strain
a_1-a_4 = coefficients

Figures 12 and 13 show two examples of verification of the proposed stress strain equations by comparing with their stress strain predictions and those of the model data. For those two figures, the solid lines represent the proposed equations while the symbols represent the NGI model data generated by PLAXIS SoilTest. There are two sets of input parameter of each figure. The data set 1 corresponds to the example case of soft clay, where input parameters are: G_{ur}/s_{uA}=200, γ_{fC}=0.04, γ_{fE}=0.15, γ_{fDSS}=0.07, s_{uA}=60 kPa, s_{uP}=24 kPa, s_{uDSS}=42 kPa. The data set 2 correspond to the example case of stiff clay, G_{ur}/s_{uA}=400, γ_{fC}=0.03, γ_{fE}=0.12, γ_{fDSS}=0.06, s_{uA}=80 kPa, s_{uP}=48 kPa, s_{uDSS}=64 kPa.

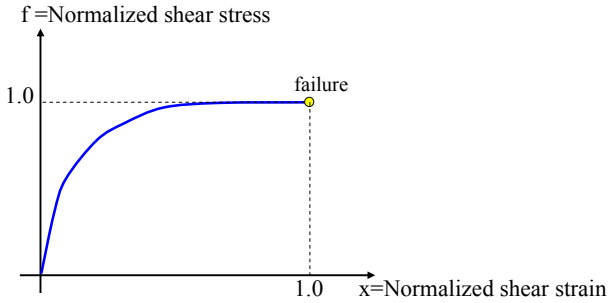

Figure 11 Schematic plot of proposed normalized stress strain curve

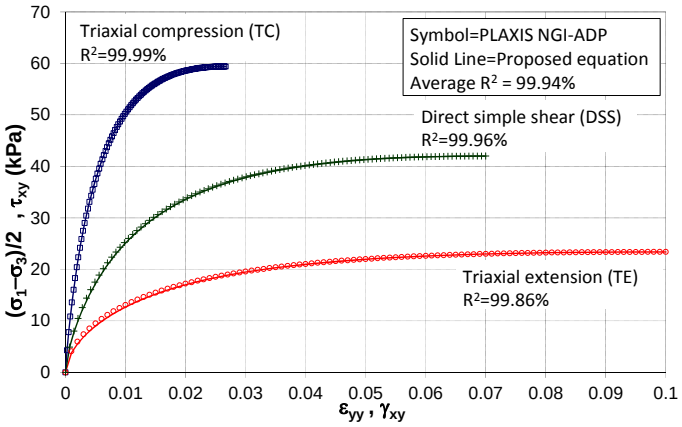

Figure 12 Comparison between proposed equations and the model data set1

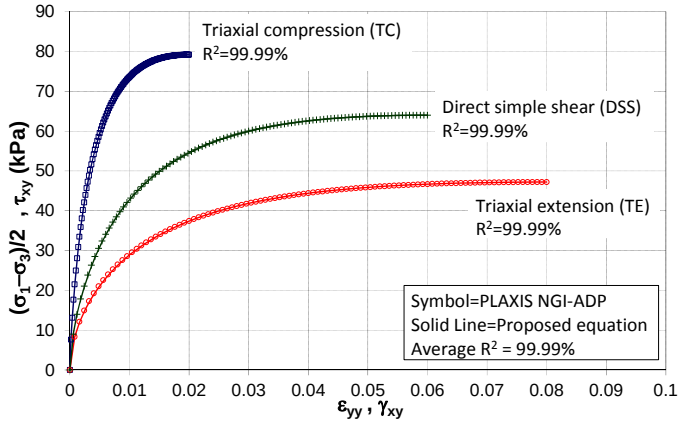

Figure 13 Comparison between proposed equations and the model data set2

It can be observed from both figures that the proposed equations of stress strain curve match the model data very accurate in all modes of shearing. High accuracy of the proposed stress strain equation is confirmed by very high value of coefficient of determination or R-squared (R^2). The R^2 values of both cases are about 99.9% for all modes of shearing and for all average results.

The proposed equations of stress strain curve of the NGI-ADP are verified for wide ranges of input parameters of G_{ur}/s_{uA}, γ_{fC}, γ_{fE}, γ_{fDSS}. All results are very satisfactory where the proposed equations accurately match with the model data for all cases which are similar to Figure 12 and 13. Very high accuracy of proposed stress strain equation is very crucial so that it will yield an accurate optimal set of input parameter when performing soil parameter optimization.

5. FORMULATION OF SOIL PARAMETER OPTIMIZATION FOR THE NGI-ADP MODEL

In this paper, there are seven decision variables, X in the soil parameter optimization as follows:

$$X = [G_{ur}, \gamma_{fC}, \gamma_{fE}, \gamma_{fDSS}, s_{uA}, s_{uP}, s_{uDSS}] \quad (12)$$

It should be noted all laboratory data concerns with initial stress state of isotropic consolidation, meaning that the input parameter of initial stress of the NGI-ADP model, K_0=1. In addition, the parameter of the effective Poisson's ratio is not optimized, but is set as constant value as: ν = 0.3, according to the typical value recommended by model formulation.

The objective function, F, of the parameter optimization is to minimize the residual sum of squares between the laboratory stress strain data (TC, TE, DSS) and associated predicted values based on proposed equation of stress strain curves presented in the previous section. Thus, the objective function has the form as:

$$\text{Residual sum of squares, } F = \sum_i (y_i - f_i)^2 \quad (13)$$

where

y_i = data set values of deviatoric stress for TC and TE and shear stress for DSS.

f_i = associated predicted of deviatoric stress for TC and TE and shear stress for DSS at the same given axial strain for TC, and TE and shear strain for DSS, based on the proposed stress strain curve in equations (8)-(10).

It should be noted that inter-relationship between s_{uTE}, s_{uP}, and s_{uA} presented in equation (7), $s_{uTE} = su_P - 0.01s_{uA}$, together with the default expression of the model, $s_{uTC}=0.99s_{uA}$ must be employed in the optimization problem in order to compute deviatoric stress for TC and TE. This is because proposed stress strain curves for triaxial compression and triaxial extension are presented in terms of shear stresses normalized by s_{uTC} and s_{uTE}, but the NGI model uses s_{uA} and s_{uP} and the model input parameter.

The optimization problem of finding the optimal set of input soil parameter of the NGI-ADP soil model leads to the least square type problem, where the residual sum of squares between the data and the prediction is minimized. Lower bound value (x_{LB}) and upper bound value (x_{UB}) of each decision variable (e.g. $X_i = [x_{LB}, x_{UB}]$) must be given in order to set up a feasible set of variable to be used in the searching region. The optimization problem has the form as:

$$\text{Minimize}(F) = \text{Minimize}\left(\sum_i (y_i - f_i)^2\right) \quad (14)$$

Subject to:
G_{ur} = [1,100000]
γ_{fC} = [0.0001,0.20]
γ_{fE} = [0.0001,0.20]
γ_{fDSS} = [0.0001,0.20]
s_{uA} = [1,300]
s_{uP} = [1,300]
s_{uDSS} = [1,300]

In this optimization problem, the shear modulus and undrained shear strengths, namely G_{ur}, s_{uA}, s_{uP}, s_{uDSS} have unit in kPa, and failure shear strains, namely γ_{fc}, γ_{fE}, γ_{fDSS} are dimensionless.

Numerical solution of the proposed soil parameter optimization can be solved using the technique of optimization, namely nonlinear least squares or nonlinear regression (e.g. Bjorck, 1996; Venkataraman, 2009). For this method, it is required that the first derivative of the function must be differentiable. Since the proposed stress strain curves in equations (8)-(10) are rational functions, they are differentiable. Accordingly, the method of nonlinear least squares can be applied. Since the objective function of minimizing sum of squared errors are nonlinear and may be nonconvex due to rational function of proposed stress strain curve, they may be many local optimal solutions which satisfies local optimality conditions. Thus, there is no guarantee that the obtained solution is the global optimal solution and hence several different initial values of decision variables must be repeatedly tried and the global optimization solution is obtained from the least of local optimal solutions.

Instead of using classical technique of local optimization such as nonlinear regression which requires derivative approach and changes of initial values of variables, solution of proposed soil parameter optimization can also be solved using the technique of global optimization (e.g. Horst et al., 2000) such as evolutionary algorithms, swarm-based optimization algorithms, or differential evolution. In this paper, the proposed optimization problem is coded in FORTRAN language and the optimal set of soil parameters is solved by the state-of-the-art solver, MIDACO (Schlueter et al. 2009; Schlueter, 2013). MIDACO is an extended ant colony optimization which is one of swarm-based optimization algorithms. The distinct feature of this solver is that it employs an evolutionary metaheuristic search strategy to determine the global optimal solution from the searching space in an intelligent and efficient way as if ants seek the best path between their colony and a source of food. The searching space is generated from multi kernel Gaussian probability density function. In addition, MIDACO is a self-adaptive algorithm to automatically determine the global optimal solution rather the local optimal solution. Thus, there is no need to change initial value of decision variables by users. Furthermore, the software does not require property of differentiability of first derivative for the nonlinear objective function or nonlinear equality or inequality constraints. Since MIDACO is a global optimization algorithm, it ensures that the solution presented in this paper corresponds to the global optimal solution of soil parameter optimization for the NGI soil model.

All analyses of soil parameter optimization were carried out on a Windows 7-based system, Intel Core I7-4770 CPU, @ 3.40 GHz and 8 GB memory.

6. PARAMETER OPTIMIZATION FOR BANKGKOK SOFT CLAY

Two sites data of Bangkok soft clay were used to determine the input soil parameters of the NGI-ADP model, including the AIT data (Khan, 1999) and the Chula data (Thongchim, 2003), shown in Table 2. The available laboratory results of these two sites include undrained shear tests of isotropic consolidation of triaxial compression (TC) and triaxial extension (TE). However, the laboratory results of undrained direct simple shear test (DSS) were unavailable for those two sites. Since the NGI-ADP soil model requires the DSS test data, the paper obtains the DSS data by assuming that they are approximated from the average stress strain curve of TC and TE tests. Research studies of Ladd (1991) and Ladd and DeGroot (2003) showed that undrained shear strength and failure strain of DSS mode falls in between those of TC and TE. Thus, it is reasonable to assume that the DSS stress strain curve should fall in between that of TC and TE, similar to undrained shear strength and failure strain.

Accordingly, the shear stress of the DSS test is simply equal to the average of shear stresses of TC and TE tests at the same given shear strain of TC and TE. The interpolation of DSS shear strain is at the interval of 0.005 for both TC and TE tests. Since the NGI model cannot describe the stress strain relationship in softening behavior, some laboratory data of stress strain curve for TC and TE having softening parts are truncated and replaced with constant values of maximum deviator stresses.

Table 2 Properties of Bangkok soft clay for parameter optimization

Soil data	AIT site	Chula site
Depth (m)	5.0-5.5	8.5-9.5
Water content, w (%)	92	62.6
Liquid limit, LL (%)	114	79
Plastic limit, PL (%)	35	37
Plasticity index, PI (%)	79	42
Specific gravity, G_s	2.7	2.68
Moisture unit weigth, γ_t (kN/m^3)	14.7	16.3
Undrained triaxial compression test (TC)	Yes	Yes
Undrained triaxial compression test (TE)	Yes	Yes
Undrained direct simple shear test (DSS)	N.A.	N.A.
Isotropic consolidation stress for TC and TE (kPa)	84	80

In order to obtain the DSS stress strain curve, the axial strain (ε_{yyTC}, ε_{yyTE}) versus deviatoric stress of TC test, $(\sigma_{yy}-\sigma_{xx})_{TC}$, and TE test, $(\sigma_{yy}-\sigma_{xx})_{TE}$ must be converted to their corresponding shear stresses (τ_{TC}, τ_{TE}) and shear strains (γ_{TC}, γ_{TE}) as:

TC shear stress: $\tau_{TC} = (\sigma_{yy}-\sigma_{xx})_{TC}/2$ (15)
TC shear strain: $\gamma_{TC} = 3\varepsilon_{yyTC}/2$ (16)
TE shear stress: $\tau_{TE} = (\sigma_{yy}-\sigma_{xx})_{TE}/2$ (17)
TE shear strain: $\gamma_{TE} = 3\varepsilon_{yyTE}/2$ (18)
Approximated DSS shear stress, $\tau_{xy} = 0.5(\tau_{TC} + \tau_{TE})$ (19)
Approximated DSS shear strain, $\gamma_{xy} = 0.5(\gamma_{TC} + \gamma_{TE})$ (20)

Figures 14 and 15 show results of stress strain curves using the proposed technique of soil parameter optimization. Computational times of soil parameter optimization using MIDACO solver for each soil data are about 1-2 minutes in order to determine the optimal set of input parameter as summarized in Table 3. It can be seen that the predicted stress strain responses and undrained shear strength match extremely well with the soil data for all tests and all sites. This excellent matching is confirmed by a very high value of average coefficient of determination, R^2 = 99.89 and 99.68% for AIT and Chula data, respectively.

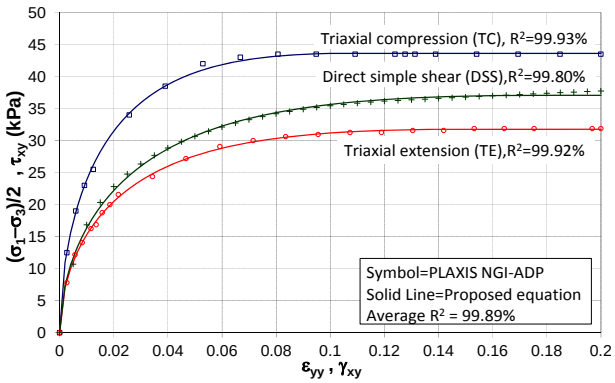

Figure 14 Results of parameter optimization of AIT site

The major advantage of using technique of soil parameter optimization is that users obtain the optimal set of input soil parameter automatically and efficiently without process of trial-and-error testing of each parameter. This technique ensures that the obtained soil parameters generate anisotropic stress strain responses and undrained shear strengths best fitted by the soil data for all undrained tests as shown in Figures 14 and15.

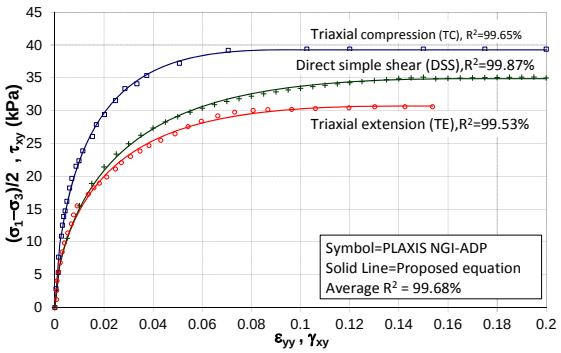

Figure 15 Results of parameter optimization of Chula site

Table 3 Optimal set of parameter for Bangkok soft clay

Parameter	AIT Site	Chula site
G_{ur}/s_{uA}	684	255
γ_{fC}	0.15	0.136
γ_{fE}	0.219	0.208
γ_{fDSS}	0.171	0.166
ν	0.3	0.3
s_{uA} (kPa)	44.1	39.7
s_{uP} (kPa)	32.2	31.1
s_{uDSS} (kPa)	37.1	34.8
τ_0/s_{uA}	0	0

7. CONCLUSION

This paper reviewed capabilities of a recent developed constitutive soil model, the NGI-ADP. The model was formulated in terms of generalized 3D state of stress and suitable for undrained deformation and stability analyses by finite element. The main feature of this model is that it can simulate anisotropic stress strain responses and strengths in generalized modes of shearing, which is completely defined by matching undrained shear strengths and failure strains in three independent shearing modes, namely TC, TE and DSS.

Parametric studies presented in this paper indicated that characteristic curvature of stress strain in each mode of shearing depended on the values of G_{ur}/s_{uA} and its corresponding shear strain γ_{fC}, γ_{fE}, γ_{DSS}. In addition, it was found that there was inter-relationship between s_{uTE}, s_{uP} and s_{uA}. Even though it seemed that direct input of undrained shear strength and failure shear strains from those tests can be made, a more fitting of stress strain curvature and strengths requires a manual trial-and-error testing of those input parameters in order to closely match with those stress strain curves.

In order to obtain the optimal set of input parameters of the NGI-ADP model efficiently without the process of a trial-and-error testing, a technique of soil parameter optimization was proposed in this paper. In addition, expressions of stress strain curves of three stress paths (TC, TE, DSS) were also proposed in conjunction with method of parameter optimization. The proposed equations could match very accurately those stress strain curves generated from the model.

Formulation of soil parameter optimization was based on statistical approach of least squares. The objective function is to minimize the residual sum of squares between the laboratory stress strain data (TC, TE, DSS) and associated predicted values based on proposed equations of stress strain curves. There are seven decision variables or soil parameters to be optimized simultaneously. The developed system of soil parameter optimization could determine the optimal set of soil parameter automatically and efficiently, where the optimal solution was solved by the global optimization solver, MIDACO.

The developed soil parameter optimization system was applied to determine the optimal set of input soil parameters of NGI-ADP model for Bangkok soft clay. Two laboratory soil data of Bangkok clay included AIT site and Chula sites. Data of DSS test were assumed to be the average between TC and TE since data of DSS was unavailable for those sites. The results showed that predicted stress strain curves could match accurately with laboratory data of all tests, including, TC, TE, DSS for two sites of Bangkok soft clay. The proposed technique of soil parameter optimization makes it possible to easily, automatically and reliably determine the optimal set of input soil parameters of the NGI-ADP model, which best fits the laboratory soil data of TC, TE, and DSS. The technique does not require manual trial-and-error testing or parametric studies of input parameters. Since this soil model is available in the finite element code, PLXIS2D, the proposed and developed technique of soil parameter optimization is valuable in determining the soil parameter of the NGI model where anisotropic undrained stress strain strengths are required in the finite element analysis of undrained ground movement and stability in geotechnical engineering practice.

8. REFERENCES

Baker, R., and Desai, C. S. (1984). "Induced anisotropy during plastic softening." Int. J. Numer. Anal. Methods Geomech., 8(2), 167–185.

Bjorck, A. (1996) Numerical methods for least squares problems, SIAM, Philadelphia.

Brinkgreve, R. B. J., PLAXIS2D, (2012), Plaxis bv, 2600 AN Delft, The Netherlands, www.plaxis.com.

Casagrande, A., and Carillo, N. (1944) "Shear failure of anisotropic soils". Contributions to Soil Mechanics (BSCE), 1941–1953, pp 122–135.

Davis, E. H., and Christian, J. T. (1971) "Bearing capacity of anisotropic cohesive soil". Journal of Soil Mechanics and Foundation Division, 97, pp 753–769.

Grimstad, G., Andresen, L., and Jostad, H. P. (2012) "NGI-ADP: Anisotropic shear strength model for clay". International Journal for Numerical and Analytical Methods in Geomechanics, 36, pp 483–497.

Horst, R., Pardalos, P. M., and Thoai N. V. (2000) Introduction to Global Optimization, Second Edition. Kluwer Academic Publishers.

Karstunen, M., Krenn, H., Wheeler, S. J., Koskinen, M., and Zentar R. (2005). "The effect of anisotropy and destructuration on the behaviour of Murro test embankment". International Journal of Geomechanics (ASCE), 5(2), pp 87–97.

Khan, R. M. (1999) "Stress-strain behavior of soft Bangkok clay below the state boundary surface under anisotropic conditions", Master thesis, Asian Institute of Technology, Bangkok, Thailand.

Koutsoftas, D. C., and Ladd C. C. (1985) "Design strengths for an offshore clay". Journal of Geotechnical Engineering, 111(3), pp 337-355.

Ladd, C. C. (1991) "Stability evaluations during stage construction". Journal of Geotechnical Engineering, 117(4), pp 540–615.

Ladd, C. C., and DeGroot D. J. (2003) "Recommended practice for soft ground site characterization: The Arthur Casagrande Lecture", Proceedings of the 12th Pan-American Conference on Soil Mechanics and Geotechnical Engineering, Boston, MA, , pp 3-57.

Li, X. S., and Dafalias, Y. F. (2004). "A constitutive framework for anisotropic sand including non-proportional loading." Géotechnique, 54(1), 41–56.

Liu, M. D., and Indraratna, N. (2011). "General strength criterion for geomaterials including anisotropic Effect." International Journal of Geomechanics, Vol. 11, No. 3, June 1, 251-262.

Oda, M., and Nakayama, H. (1988). "Introduction to inherent anisotropy of soils in the yield function." Micromechanics of granular materials, M. Satake and J. Jenkins, eds., Elsevier Science, Amsterdam, The Netherlands, 81–90.

Pestana, J. M., Whittle, A. J., and Gens, A. (2002) "Evaluation of a constitutive model for clays and sands, Part II, Clay behaviour". International Journal for Numerical and Analytical Methods in Geomechanics, 26(11), pp1097-1121.

Potts, D. M., and Zdravkovic, L. (1999) Finite Element Analysis in Geotechnical Engineering: Theory, Thomas Telford Publishing, pp 143-146.

Seah, T. H. (1990) "Anisotropy of normally consolidated Boston blue clay", Sc.D. Thesis, Massachusetts Institute of Technology, Boston, U.S.A.

Su, S. F., Liao, H. J., and Lin, Y. H. (1998) "Base stability of deep excavation in anisotropic soft clay". Journal of Geotechnical and Geoenvironmental Engineering, 124(9), pp 809–819.

Sambhandharaksa, S. (1977). Stress-strain-strength anisotropy of varved clays, Doctoral thesis, Massachusetts Institute of Technology, Boston, U.S.A.

Schlueter, M., Egea, J. A., and Banga, J. R. (2009) "Extended ant colony optimization for non-convex mixed integer nonlinear programming". Computer Operation Research 36(7), pp 2217–2229.

Schlueter, M. (2013). MIDACO, Global optimization software for mixed integer nonlinear programming. Software available at http://www.midaco-solver.com, 2013..

Shibuya, S., Hight, D. W., and Jardine, R. J. (2003). "Four dimensional local boundary surfaces of an isotropically consolidated loose sand." Soils Found., 43(2), 89–103.

Thongchim, P. (2003) "Effect of rates of cyclic loading on the mechanical behavior of soft Bangkok clay". Master thesis, Chulalongkorn university, Bangkok, Thailand.

Ukritchon, B., Whittle, A. J., and Sloan S. W. (2003) "Undrained stability of braced excavations in clay". Journal of Geotechnical and Geoenvironmental Engineering, 129(8), pp 738–755.

Venkataraman, P. (2009) Applied optimization with MATLAB Programming, John Wiley & Sons, Hoboken, NJ.

Whittle, A. J. (1993) "Evaluation of a constitutive model for overconsolidated clays". Geotechnique, 43(2), pp 289–313.

Wong, R. C. S., and Arthur, J. R. F. (1986). "Induced and inherent anisotropy." Géotechnique, 36(4), 471–481.